Escola de Primavera de Transição e Turbulência
Blumenau 2020

ABCM Associação Brasileira de Engenharia e Ciências Mecânicas

12th Spring School on Transition and Turbulence
September 21st-25th, 2020, Blumenau, SC, Brazil

EPTT-2020-0036
THE WIND DYNAMIC PRESSURE EXERTED ON A BUILDING FACADE: NUMERICAL SIMULATION × NORMATIVE SPECIFICATIONS

Rhayssa Maryell Marra Ribas*
Vivian Machado†
Yara de Souza Tadano‡
Luiz Eduardo Melo Lima§
Department of Mechanics, Federal University of Technology—Paraná—, Ponta Grossa, PR 84017-220, Brazil
*rhayssa@alunos.utfpr.edu.br,†vivian_machadoo@yahoo.com.br,‡yaratadano@utfpr.edu.br,§lelima@utfpr.edu.br

Abstract. *The buildings' height is a determining factor in urban areas of high demographic density, considering the increase in population and the decrease in non-built habitable regions. Currently, there are Brazilian Standards (NBR) that present definitions and mathematical models for the design of safe and reliable building structures. The NBR 6123 determines calculation procedures to obtain the efforts caused by the winds under the buildings. Therefore, this work aims to compare the data provided by NBR 6123 concerning the results obtained by numerical simulations. The numerical simulations were performed by the commercial software ANSYS® Fluent®, which uses the finite volume method to solve the governing equations. The Reynolds-averaged Navier–Stokes equations were solved employing the standard k–ϵ turbulence model and the semi-implicit method for pressure linked equations algorithm for the pressure–velocity coupling. The results obtained for the pressures caused in the windward (the side where the wind blows) of a slender building showed a satisfactory concordance. Normative specifications are limited, but sufficient for the project without the need for additional experimental data. However, numerical simulations provide much more details for the project.*

Keywords: *numerical simulations, normative specifications, buildings*

1. INTRODUCTION

With the growth of large cities and the increase in population in the urban area, the creation of increasingly higher buildings has become an alternative to meet the population's need to live or own commercial properties in strategic locations close to the city center. Increasingly taller buildings are produced daily in large cities, and the advancement in material technology makes it possible to use lighter and thinner structures. The use of glass also presents itself as an alternative, driven by the creation of increasingly audacious architectures.

In this context, the knowledge of the pressures exerted by the winds in the buildings is a determining factor to avoid accidents and carry out safe projects. Wind action in buildings has been one of the main circumstances that limit the height of the building. When reaching high structures, the wind can produce two undesirable phenomena, a low-frequency excitation, and an excessive heat transfer. These two phenomena generate thermal discomfort, nausea, and insecurity. It is necessary to know the intensity of the forces acting on a building so that it is feasible to avoid or reduce possible oscillations (Li *et al.*, 2018).

With the help of NBR 6123 (ABNT, 1988), it is possible to estimate the efforts due to the winds in buildings. The calculation procedure is simple and involves the determination of factors such as the characteristic velocity, dynamic pressure, and static forces. Statistical, topographic factors, meteorological parameters, among others, are employed to determine these factors.

An alternative to obtaining pressures and other flow data around buildings is to carry out experiments in wind tunnels, using sensors to acquire these data. However, in addition to the need for a suitable experimental apparatus, modeling in wind tunnels requires the production of a satisfactory model and on a structural scale faithful to the original model. And often, similar operating conditions are difficult to obtain (Davenport, 1961).

Another solution for obtaining data related to flows around buildings corresponds to the use of numerical techniques, involving simulation software. This alternative requires only computational processing capacity and the use of a reliable tool with input data and models similar to real conditions.

Often, the resistance and the wind action that generates unwanted forces on the structures are the factors that limit the development of new designs and the use of different materials in high constructions. From the structural analysis, limiting values are defined that are sufficiently accurate to allow the creation of buildings maximizing safety and minimize the material cost. The use of specific rules for calculations is often limited to obtaining maximum values or even superficial

analysis of the phenomena that involve the action of winds in buildings. In this context, the use of computational fluid dynamics (CFD) tools can present itself as an alternative for more detailed and complete analyzes of the wind action in buildings, for example. With the constant advancement of computer processing technology, it is possible to perform simulations of real cases with just the click of a few buttons, whose execution of an experiment would require hours of work and financial resources. CFD software can be applied to simulate cases as the wind tunnels. This kind of tool is an alternative for modeling flows around buildings, allowing the analysis and visualization of flow profiles, as well as obtaining properties involving the phenomena (Fontella, 2014).

The basis of CFD modeling consists of the numerical solution of the governing equations of fluid mechanics (continuity, Navier–Stokes, and energy) and dispersion equations (substances concentration). Also, equations of state are defined based on considerations of thermodynamic equilibrium and Newtonian fluids (Vardoulakis *et al.*, 2003). The equations that describe the transport phenomena are continuous equations in the spatial domain, as well as in time, requiring their discretization to obtain the numerical solution (Fiates, 2015). The use of CFD allows the designer to improve and optimize his product for that application, especially in complex geometries. Due to the ease of complex problems discretization, the use of CFD allows a prototype to interact more quickly, making it possible to predict the separation of the boundary layer and the pressure center without the need for the use of a wind tunnel (Beaumont *et al.*, 2018).

Several methodologies were employed in the literature to analyze the influence of the wind on structures: finite element method (Handa and Clarkson, 1971); spatial functions (Davenport, 1995); numerical simulation and wind tunnel (Juhásová, 1997); wind tunnel (Liang *et al.*, 2002; Churin *et al.*, 2016; Tamura *et al.*, 2017); computational simulation (Khallaf and Jupp, 2017); among others.

This work aims to compare the data provided by NBR 6123 concerning the results obtained by numerical simulations of a building. The numerical simulations were performed using a commercial CFD software, which uses the finite volume method to solve the governing equations. The simulated geometry corresponds to a square-based building located on unobstructed terrain.

2. THEORETICAL REFERENTIAL

Published in June 1988 by the Brazilian Technical Standards Association (ABNT, from Portuguese: Associação Brasileira de Normas Técnicas), NBR 6123—Forces due to wind in buildings—presents methodologies used in calculating the determination of forces in buildings, due to the static and dynamic actions of the wind. This standard also indicates the use of experimental results obtained in wind tunnels, which have characteristics similar to natural wind. Two important parameters are presented in this standard: wind dynamic pressure and static forces. Factors such as topography and surface roughness of the terrain, dimensions, and use of the building, are decisive in the calculation (ABNT, 1988).

2.1 Wind dynamic pressure

The wind dynamic pressure acting on a surface can be obtained from fluid mechanics concepts, based on simplifications of the motion equation for the flow of a fluid without friction (Euler equation). The dynamic pressure (p_{dyn}) is proportional to the square of the velocity (V), air density (ρ), and ground-surface pressure coefficient (c_p)—represents the fraction of the eave-height wind dynamic pressure that is felt on the soil surface—, as expressed by Eq. (1).

$$p_{\mathrm{dyn}} = \frac{1}{2}\rho V^2 c_p \tag{1}$$

NBR 6123 presents in Sect. 4.2.c an equivalent formula to that presented in Eq. (1). Hence, the dynamic pressure (q) is dependent only on the square of the wind characteristic velocity (V_K) and a constant, as expressed by Eq. (2):

$$q = 0.613 V_K^2 \tag{2}$$

Equation (3) express the wind characteristic velocity (V_K) considering the wind basic velocity (V_0) and three dimensionless factors (S_1, S_2, and S_3):

$$V_K = V_0 S_1 S_2 S_3 \tag{3}$$

The three dimensionless factors, S_1, S_2, and S_3, are determined in Sects. 5.2, 5.3, and 5.4 of the NBR 6123, respectively. S_1 is a topographic factor, S_2 is a factor related to the terrain roughness, and S_3 is a statistical factor depending on the type of building and its occupation.

By definition, the wind basic velocity value, V_0, is considered as the velocity of a gust of 3 s, exceeded on average once during the useful life period considered for structures, which is 50 years. The height considered for the velocity incidence is 10 m above the terrain, considering an opened flat field. Hence, to obtain V_0, it is necessary to consult an isopleth graph (Fig. 1), as presented by Padaratz (1977), and later inserted in NBR 6123 (ABNT, 1988).

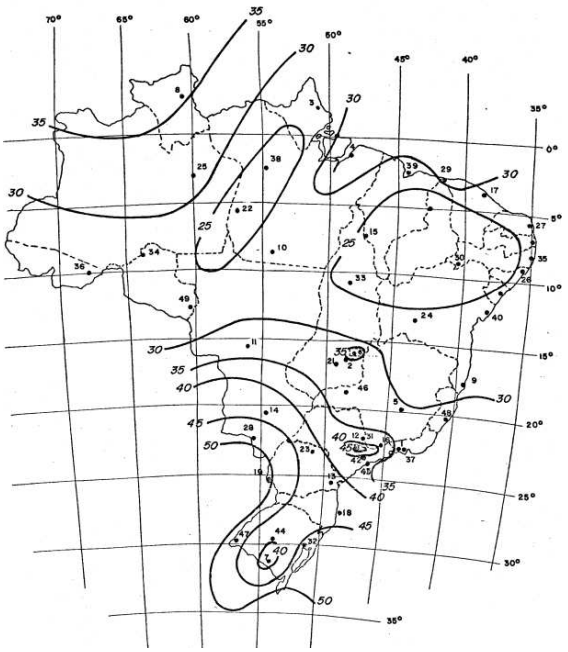

Figure 1. Isopleths maps of the Brazil (Padaratz, 1977).

3. MODEL

This section presents the definitions of the governing equations (Sect. 3.1) and the turbulence model (Sect. 3.2) for the computational model employed in this work.

3.1 Governing equations

Equations (4), (5), and (6) are the RANS equations and express the conservation of mass, momentum, and energy, respectively, in steady-state for incompressible flow (Tannehill *et al.*, 1997):

$$\frac{\partial \overline{u}_j}{\partial x_j} = 0 \tag{4}$$

$$\frac{\partial}{\partial x_j}\left(\rho \overline{u}_i \overline{u}_j + \widehat{p}\delta_{ij} - \overline{\tau}_{ij}^{\mathrm{tot}}\right) = 0 \tag{5}$$

$$\frac{\partial}{\partial x_j}\left[\left(\rho C_p \overline{T} - \widehat{p}\right)\overline{u}_j - \overline{\tau}_{ij}^{\mathrm{tot}}\overline{u}_i + \overline{q}_j^{\mathrm{tot}}\right] = 0 \tag{6}$$

Where x_i and $\overline{u}_i$ represent the position and velocity vectors, respectively, δ_{ij} is the Kronecker delta function, ρ is the density, C_p is the isobaric specific heat, and $\overline{T}$ is the absolute temperature.

The modified pressure $\widehat{p}$ has its definition given by Eq. (7):

$$\widehat{p} = \overline{p} + \rho g x_i \tag{7}$$

Where g is the gravitational acceleration. For an ideal gas, the static pressure is provided by $\overline{p} = \rho R \overline{T}$, with R being the gas constant.

The total (laminar and turbulent) viscous stress, $\overline{\tau}_{ij}^{\mathrm{tot}}$, and the total (laminar and turbulent) heat flux, $\overline{q}_j^{\mathrm{tot}}$, are given by Eqs. (8) and (9), respectively:

$$\overline{\tau}_{ij}^{\mathrm{tot}} \equiv \overline{\tau}_{ij}^{\mathrm{lam}} + \overline{\tau}_{ij}^{\mathrm{turb}} = (\mu + \mu_{\mathrm{t}})\left(\frac{\partial \overline{u_i}}{\partial x_j} + \frac{\partial \overline{u_j}}{\partial x_i}\right) \tag{8}$$

$$\overline{q}_j^{\mathrm{tot}} \equiv \overline{q}_j^{\mathrm{lam}} + \overline{q}_j^{\mathrm{turb}} \approx -C_p\left(\frac{\mu}{\mathrm{Pr}} + \frac{\mu_{\mathrm{t}}}{\mathrm{Pr}_{\mathrm{t}}}\right)\frac{\partial \overline{T}}{\partial x_j} \tag{9}$$

Where μ and μ_{t} are the molecular and turbulent dynamic viscosities, respectively, and Pr and Pr_{t} are the laminar and turbulent Prandtl numbers, respectively.For air $\mathrm{Pr} \approx 0.71$, and a turbulence model is used to give values for μ_{t} as well as Pr_{t}, although $\mathrm{Pr}_{\mathrm{t}} \approx 0.9$ is usually employed.

3.2 Turbulence model

The standard k–ϵ turbulence model proposed by Launder and Spalding (1974) consists of the two transport equations. The first for the turbulent kinetic energy k, Eq. (10), and the second for its dissipation rate ϵ, Eq. (11):

$$\frac{\partial}{\partial t}(\rho k) + \frac{\partial}{\partial x_j}\left[\rho k u_j - \left(\mu + \frac{\mu_\mathrm{t}}{\sigma_k}\right)\frac{\partial k}{\partial x_j}\right] = P_k + P_\mathrm{b} - Y_\mathrm{Ma} - \rho\epsilon \tag{10}$$

$$\frac{\partial}{\partial t}(\rho \epsilon) + \frac{\partial}{\partial x_j}\left[\rho \epsilon u_j - \left(\mu + \frac{\mu_\mathrm{t}}{\sigma_\epsilon}\right)\frac{\partial \epsilon}{\partial x_j}\right] = C_{1\epsilon}\left(P_k + C_{3\epsilon}P_\mathrm{b}\right)\frac{\epsilon}{k} - C_{2\epsilon}\rho\frac{\epsilon^2}{k} \tag{11}$$

Where σ_k and σ_ϵ are the turbulent Prandtl numbers for k and ϵ, respectively, and these constants are in Table 1. For steady-state, the time derivatives in Eqs. (10) and (11) can be eliminated, i.e., $\partial/\partial t = 0$.

The turbulent viscosity, μ_t, is calculated by combining k and ϵ, according to Eq. (12):

$$\mu_\mathrm{t} = C_\mu \rho \frac{k^2}{\epsilon} \tag{12}$$

Where C_μ is a constant, and its value is in Table 1.

The kinetic energy production term due to the mean velocity gradients, P_k, is given by Eq. (13):

$$P_k = -\rho\overline{u_i' u_j'}\frac{\partial u_j}{\partial x_i} \equiv \mu_\mathrm{t} S^2 \tag{13}$$

Where S ($\equiv \sqrt{2S_{ij}S_{ij}}$) is the modulus of the mean rate-of-strain tensor considering the Boussinesq hypothesis, i.e., $S_{ij} = (1/2)(\partial u_i/\partial x_j + \partial u_j/\partial x_i)$.

The kinetic energy production term due to buoyancy, P_b, is given by Eq. (14):

$$P_\mathrm{b} = g_i \beta \frac{\mu_\mathrm{t}}{\mathrm{Pr}_\mathrm{t}}\frac{\partial T}{\partial x_i} \tag{14}$$

Where g_i is the gravitational acceleration vector. For the standard k–ϵ model, the Pr_t default value is 0.85. By definition, the thermal expansion coefficient is $\beta = -(1/\rho)(\partial\rho/\partial T)_p$. For isothermal flow, the kinetic energy production term due to buoyancy can be eliminated, i.e., $P_\mathrm{b} = 0$.

The dilatation dissipation term, Y_Ma, is modeled by Eq. (15), according to Sarkar and Lakshmanan (1991):

$$Y_\mathrm{Ma} = 2\mathrm{Ma}_\mathrm{t}^2 \rho\epsilon \tag{15}$$

Where the turbulent Mach number is defined as $\mathrm{Ma}_\mathrm{t} = \sqrt{k/a^2}$, by definition, and a ($\equiv \sqrt{\gamma RT}$, for an ideal gas) is the speed of sound, with γ being the specific heats' ratio, and R is the gas constant. For incompressible flow, the dilatation dissipation term can be eliminated, i.e., $Y_\mathrm{Ma} = 0$.

Table 1 presents the default values of the coefficients in the standard k–ϵ model selected in the computational tool.

Table 1. Default values of the coefficients in the standard k–ϵ model.

$C_{1\epsilon}$	$C_{2\epsilon}$	$C_{3\epsilon}$	C_μ	σ_k	σ_ϵ
1.44	1.92	[a]	0.09	1.0	1.3

[a] $0 \leq C_{3\epsilon} \leq 1$, but an approximation that satisfies both limits is $C_{3\epsilon} = \tanh|v/u|$, where v and u are the velocity components parallel and perpendicular to the gravitational vector, respectively (Henkes *et al.*, 1991).

4. NUMERICAL PROCEDURE

The commercial software ANSYS® Fluent® Release 18.2 was employed to run the numerical simulations in this work. All steady-state simulations were performed using a finite volume method (Patankar, 1980) with a non-structured and non-uniform mesh. The pressure–velocity coupling was solved using the semi-implicit method for pressure linked equations (SIMPLE) algorithm (Patankar, 1980). The "Enhanced Wall Treatment" option was selected that provides consistent solutions for all y^+ values and is recommended when using the k–ϵ turbulence model for general single-phase fluid flow problems (ANSYS, 2017). The following schemes have been considered in the simulations performed:

- Second-order for pressure.
- Second-order upwind for momentum.
- First-order upwind for turbulent kinetic energy and its dissipation rate.

All simulations are performed in the Computational Research Laboratory, linked to the Graduate Program in Mechanical Engineering of the Federal University of Technology—Paraná—, using a computer with the following characteristics:

- Microsoft Windows® 7 (64-bit) operating system.
- Intel® Core™ i7–7500 (2.7 GHz) processor.
- 8 GB RAM.

The following sections introduce the descriptions and characteristics of the building geometry and computational domain (Sect. 4.1), as well as the computational mesh (Sect. 4.2), considered in the numerical procedure.

4.1 Building geometry and computational domain

A building with a square base $L \times L$ (25 m $\times$ 25 m) and 50 m height H (about 16 floors), located on the terrain without obstacles, was the central object of the computational domain, as shown in Fig. 2. The wind velocity profile was supposed uniform and employed as an input parameter, using the characteristic velocity value calculated by NBR 2163, to get a comparison between the methods of obtaining the results. The boundary conditions employed in the simulations are also shown in Fig. 2.

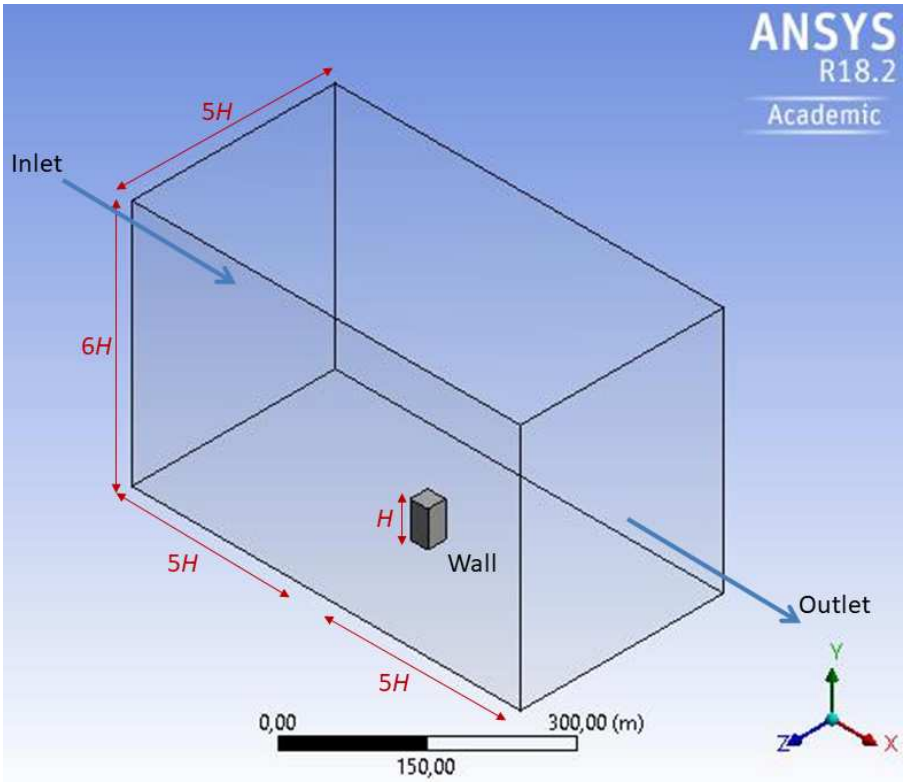

Figure 2. Building geometry and computational domain.

The "Enclosure tool", available in the ANSYS® DesignModeler™ software, was employed to create the computational domain, where it is possible to insert a geometry (body) inside a domain of pre-established dimensions and formats.

For domain simulations containing only one building, $6H$ vertical values are recommended, to ensure reliable assessments of the characteristics present above the upper limit of the buildings and to prevent the artificial acceleration of the flow above the buildings (Blocken *et al.*, 2004). Also, the application of a factor is considered for side dimensions evaluation. This factor is called "Blockage", defined as the ratio between the building projected area towards the wind and the computational domain free section. Hence, low "Blockage" values suggest the use of lateral distances between the building and the boundaries of the $5H$ domain, considering isolated structures (Franke *et al.*, 2007). Lastly, to define the domain dimension considering the flow direction (longitudinal), $5H$ distances between the border and the wall of a single building are indicated (Scaperdas and Gilham, 2004). Figure 2 shows these dimensions.

4.2 Computational mesh

The ANSYS® Meshing™ tool was applied to generate the computational mesh. The computational mesh used in the numerical simulations is of the uniform linear type. First, a coarse mesh was generated, and a visual evaluation was performed according to the element quality. Then, a general mesh refinement was carried out across the domain to obtain a higher elements' number with better quality. Figure 3 shows the comparison between the quality classification of the two meshes generated, where values closer to 1 are better.

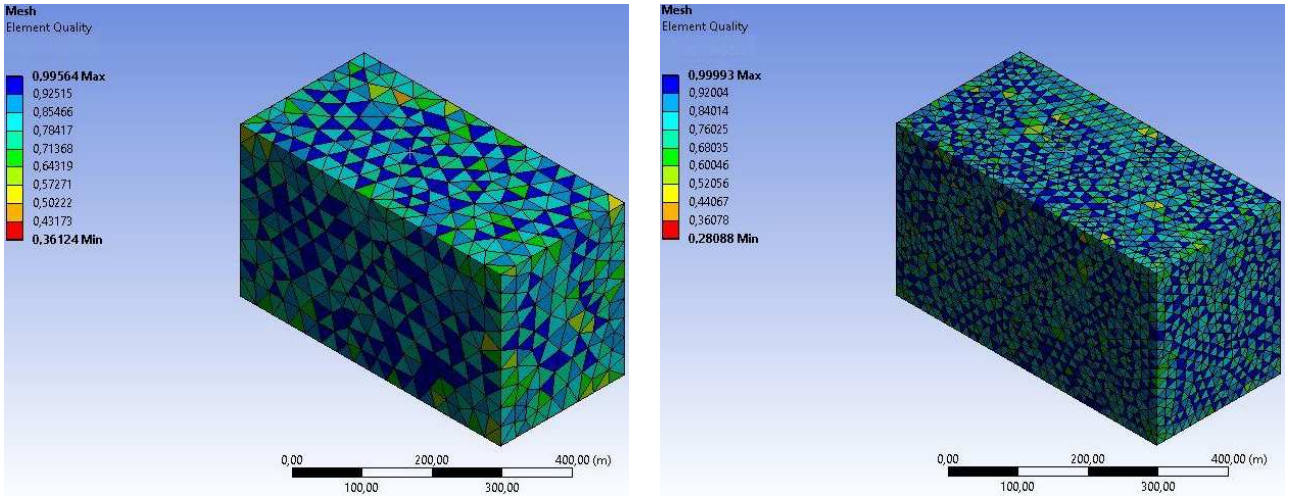

(a) (b)

Figure 3. 3D computational meshes analyzed: (a) coarse and (b) refined.

The coarse mesh has 1700 nodes and 7825 elements, and the refined mesh has 8484 nodes and 41831 elements. The mesh used in the simulation was the refined mesh, shown in the side view in Fig. 4.

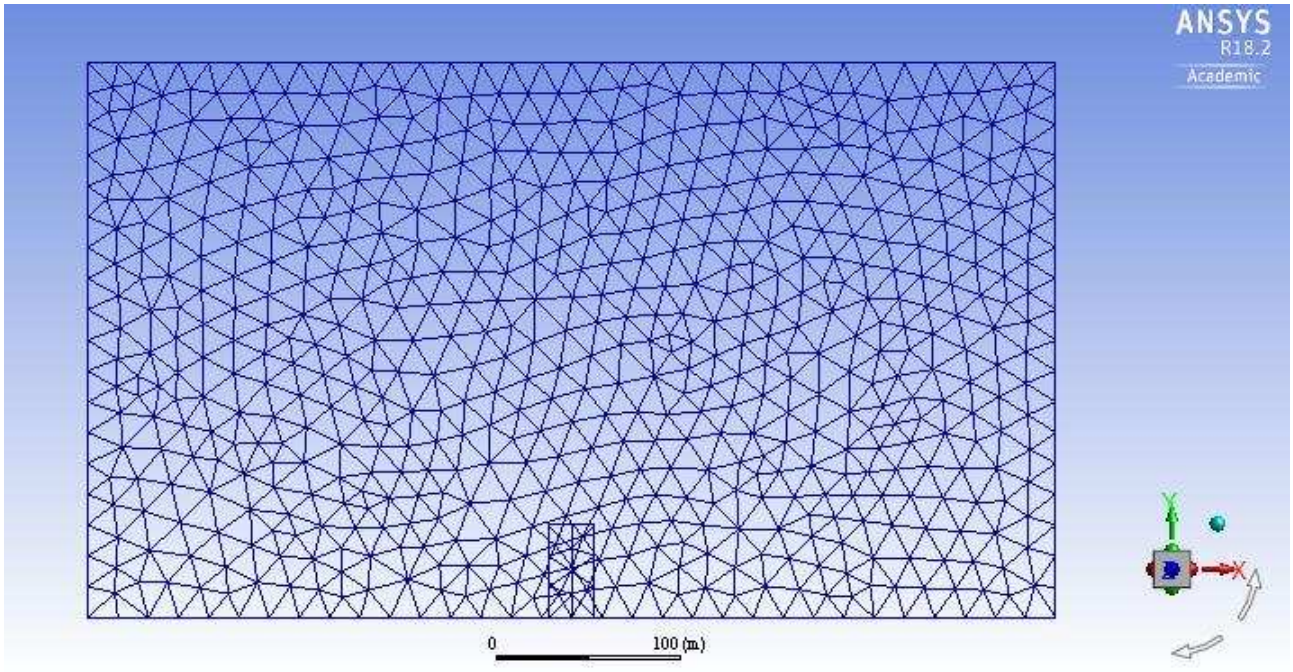

Figure 4. Side view of the 3D computational mesh used.

5. RESULTS AND DISCUSSION

This section presents the wind dynamic pressure calculation (Sect. 5.1) and simulations results (Sect. 5.2) performed in this work.

5.1 Wind dynamic pressure calculation

For dynamic pressure calculations, according to NBR 6123, the following considerations were performed, concerning the location and characteristics of the building:

- Small town, with densely built suburb, in the state of Paraná.
- Flat terrain.
- Building with a high occupancy factor (commerce, hotel, or residence).

A summary of the factors used, together with the results applied in Eqs. (2) and (3), are shown in Table 2. The correction factors presented are useful for improving the local conditions of the building, thus adjusting the turbulent conditions and the limits implicit in NBR 6123.

Table 2. Parameters used for the simulations.

Parameter	Symbol	Value used/calculated	Unit
Topographic factor	S_1	1	–
Roughness factor	S_2	0.96	–
Statistical factor	S_3	1	–
Wind basic velocity	V_0	45	m/s
Wind characteristic velocity	V_K	43	m/s
Dynamic pressure	q	1133.59	Pa

5.2 Simulations results

After 461 iterations, the solution showed convergence considering residues less than 10^{-4}, for continuity, 10^{-7}, for velocity, 10^{-4}, for turbulent kinetic energy, and 10^{-6}, for turbulent kinetic energy dissipation.

Figure 5a–b presents the numerical results obtained for the dynamic pressure distribution (or field) in the side and perspective views, respectively. The maximum value obtained on the windward side of the building, represented by the orange color in Fig. 5, was 1175.23 Pa, whose value is close to the value obtained by the NBR 6123 (Table 2). This result indicates that the factors S_1, S_2, and S_3 generalize and linearize factors in a way that accelerates the calculation and maintains a safety margin.

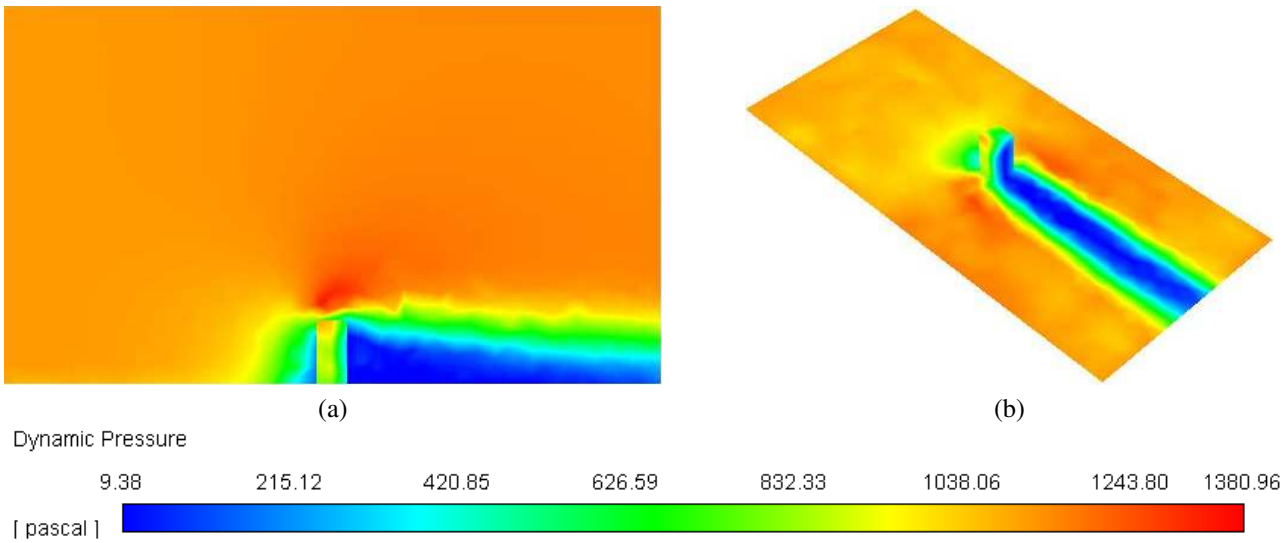

Figure 5. Dynamic pressure field: (a) side view and (b) perspective view.

Figure 6a–b presents the numerical results obtained for the dynamic pressure distribution (or field) in the side and top views, respectively. The total pressure acting in the building was 1223.37 Pa, slightly above the dynamic pressure value obtained by the NBR 6123 (Table 2). It is important to note that the Y-axis in Fig. 6a was reduced for this representation since it did not present a significant gradient.

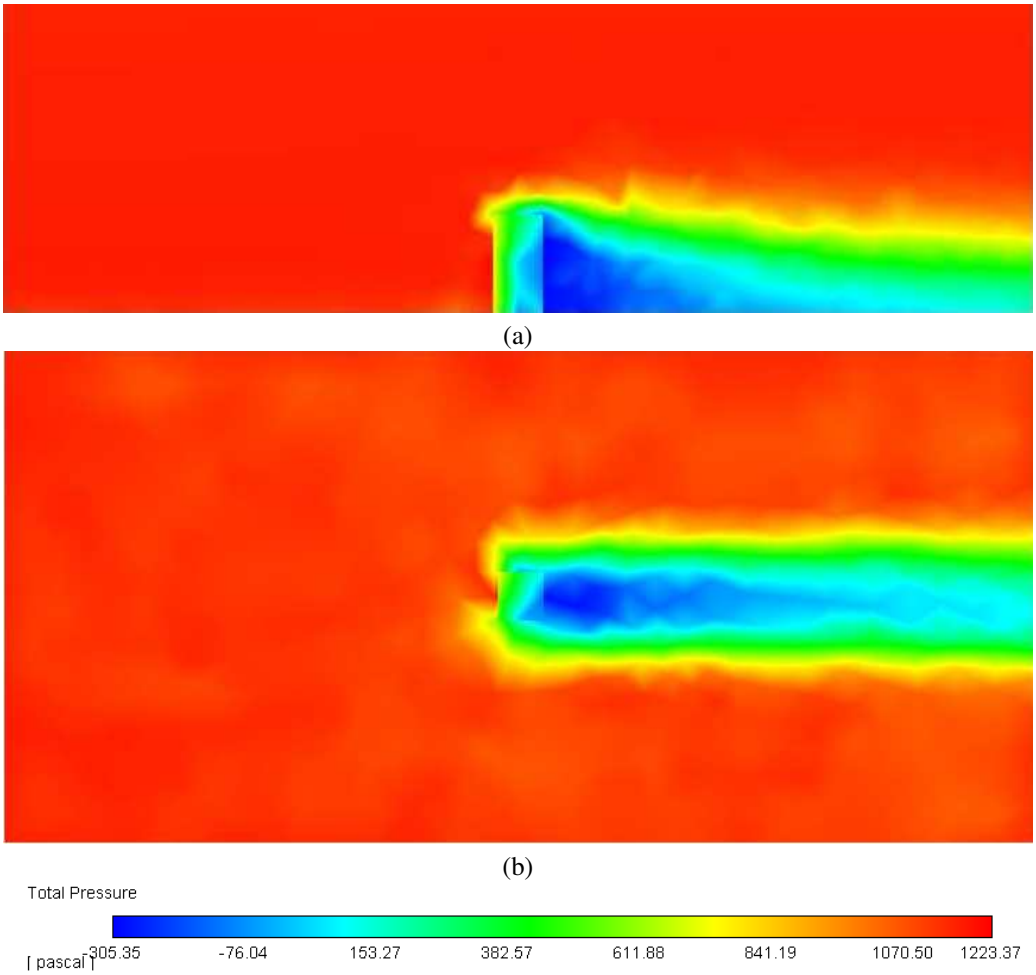

Figure 6. Total pressure field: (a) side view and (b) top view.

Figure 7 shows the numerical results obtained for the velocity vectors distribution (or field). It is possible to observe the details of the formation of vortices in the building's roof (the opposite part that the wind blows). Also, there is an acceleration of flow when coming into contact with the upper boundary of the construction. The entry velocity profile was supposed uniform, since the value used in the NBR 6123 calculations is also constant, and the simulations must reproduce the same case considered by NBR 6123. It is important to note that the Y-axis in Fig. 7 was reduced for this representation since it also did not present a significant gradient.

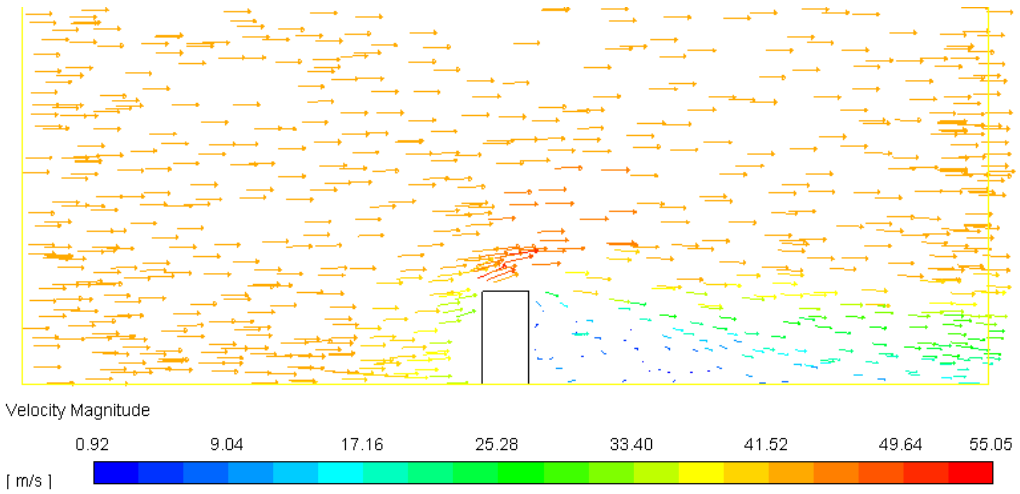

Figure 7. Velocity vectors field.

6. CONCLUSIONS

The use of NBR 6123 provides a quick and simple calculation, eliminating the need for a wind tunnel study. However, the geometries considered in the standard are limited and use generalized correction factors for the velocity due to the occurrence of a boundary layer and the turbulence generated by the relief. Also, the standard considers a base velocity as the velocity of a gust of 3 s, 10 m above the terrain, exceeded on average once during 50 years, being above the efforts applied to buildings.

Thus, the standard is very conservative and serves to determine the resulting force in more practical engineering cases, and only specifies what the maximum efforts will be. On the other hand, the numerical analysis provides more detailed results, discovering pressure profiles applied on surfaces that can be optimized to reduce efforts, among other important parameters. For example, the vortex wake generation, pollutant dispersion, as well as other relevant parameters to the building construction.

Finally, to reduce the simulation time, it is possible to use reduced computational domains, considering cases similar to the simulated. A $3H$ height was sufficient to not display significant variations in the Y-axis. Also, this domain size reduction allows for an increase in mesh refinement, maintaining a similar computational effort. Additionally, the use of a user-defined function that can provide a more realistic velocity profile (i.e., power-law) could produce more satisfactory results in the simulations.

7. ACKNOWLEDGEMENTS

The authors thank the Federal University of Technology—Paraná—for the resources made available.

8. REFERENCES

ABNT, 1988. *NBR 6123: Forças devidas ao vento em edificações*. Associação Brasileira de Normas Técnicas (ABNT), Rio de Janeiro, RJ. In Portuguese.

ANSYS, 2017. *ANSYS Fluent Tutorial Guide*. ANSYS, Inc., Canonsburg, PA. Release 18.0.

Beaumont, F., Taiar, R., Polidori, G., Trenchard, H. and Grappe, F., 2018. "Aerodynamic study of time-trial helmets in cycling racing using CFD analysis". *J. Biomech.*, Vol. 67, pp. 1–8. ISSN 0021-9290. DOI 10.1016/j.jbiomech.2017.10.042.

Blocken, B., Roels, S. and Carmeliet, J., 2004. "Modification of pedestrian wind comfort in the Silvertop Tower passages by an automatic control system". *J. Wind Eng. Ind. Aerodyn.*, Vol. 92, No. 10, pp. 849–873. ISSN 0167-6105. DOI 10.1016/j.jweia.2004.04.004.

Churin, P., Pomelov, V. and Poddaeva, O., 2016. "The research of wind loads on buildings and structures with increased level of responsibility". *Procedia Eng.*, Vol. 153, pp. 550–555. ISSN 1877-7058. DOI 10.1016/j.proeng.2016.08.189.

Davenport, A.G., 1961. "The application of statistical concepts to the wind loading of structures". *Proc. Inst. Civ. Eng.*, Vol. 19, No. 4, pp. 449–472. ISSN 1753-7789. DOI 10.1680/iicep.1961.11304.

Davenport, A.G., 1995. "How can we simplify and generalize wind loads?" *J. Wind Eng. Ind. Aerodyn.*, Vol. 54-55, pp. 657–669. ISSN 0167-6105. DOI 10.1016/0167-6105(94)00079-S.

Fiates, J., 2015. *Desenvolvimento de uma metodologia para simulação de dispersão de gás inflamável por meio de CFD utilizando OpenFOAM*. Master's thesis, Faculdade de Engenharia Química, Universidade Estadual de Campinas, Campinas, SP. URL `http://repositorio.unicamp.br/jspui/handle/REPOSIP/266013`. In Portuguese.

Fontella, C.R.d.F., 2014. *Análise numérica do escoamento turbulento em área urbana empregando simulação de grandes escalas*. Master's thesis, Escola de Engenharia, Universidade Federal do Rio Grande do Sul, Porto Alegre, RS. URL `https://lume.ufrgs.br/handle/10183/103817`. In Portuguese.

Franke, J., Hellsten, A., Schlünzen, H. and Carissimo, B., 2007. "Best practice guideline for the CFD simulation of flows in the urban environment". In *COST action 732 — Quality Assurance and Improvement of Microscale Meteorological Models*, Centre for Marine and Atmospheric Sciences, Meteorological Institute, University of Hamburg, Hamburg. ISBN 9783000183126.

Handa, K.N. and Clarkson, B.L., 1971. "Application of finite element method to the dynamic analysis of tall structures". *J. Sound Vib.*, Vol. 18, No. 3, pp. 391–403. ISSN 0022-460X. DOI 10.1016/0022-460X(71)90710-3.

Henkes, R.A.W.M., Van Der Vlugt, F.F. and Hoogendoorn, C.J., 1991. "Natural-convection flow in a square cavity calculated with low-Reynolds-number turbulence models". *Int. J. Heat Mass Transfer*, Vol. 34, No. 2, pp. 377–388. ISSN 0017-9310. DOI 10.1016/0017-9310(91)90258-G.

Juhásová, E., 1997. "Quasi-static versus dynamic space wind response of slender structures". *J. Wind Eng. Ind. Aerodyn.*, Vol. 69-71, pp. 757–766. ISSN 0167-6105. DOI 10.1016/S0167-6105(97)00203-1.

Khallaf, M. and Jupp, J., 2017. "Performance-based design of tall building envelopes using competing wind load and wind flow criteria". *Procedia Eng.*, Vol. 180, pp. 99–109. ISSN 1877-7058. DOI 10.1016/j.proeng.2017.04.169.

Launder, B.E. and Spalding, D.B., 1974. "The numerical computation of turbulent flows". *Comput. Methods Appl. Mech.*

Eng., Vol. 3, No. 2, pp. 269–289. ISSN 0045-7825. DOI 10.1016/0045-7825(74)90029-2.

Li, Y., Tian, X., Tee, K.F., Li, Q.S. and Li, Y.G., 2018. "Aerodynamic treatments for reduction of wind loads on high-rise buildings". *J. Wind Eng. Ind. Aerodyn.*, Vol. 172, pp. 107–115. ISSN 0167-6105. DOI 10.1016/j.jweia.2017.11.006.

Liang, S., Liu, S., Li, Q.S., Zhang, L. and Gu, M., 2002. "Mathematical model of acrosswind dynamic loads on rectangular tall buildings". *J. Wind Eng. Ind. Aerodyn.*, Vol. 90, No. 12-15, pp. 1757–1770. ISSN 0167-6105. DOI 10.1016/S0167-6105(02)00285-4.

Padaratz, I.J., 1977. *Velocidade básica do vento no Brasil*. Master's thesis, Escola de Engenharia, Universidade Federal do Rio Grande do Sul, Porto Alegre, RS. URL `https://lume.ufrgs.br/handle/10183/11976`. In Portuguese.

Patankar, S.V., 1980. *Numerical Heat Transfer and Fluid Flow*. Series in Computational Methods in Mechanics and Thermal Sciences. Hemisphere Publ. Co., New York, NY, 1st edition. ISBN 9780891165224.

Sarkar, S. and Lakshmanan, B., 1991. "Application of a Reynolds stress turbulence model to the compressible shear layer". *AIAA J.*, Vol. 29, No. 5, pp. 743–749. ISSN 1533-385X. DOI 10.2514/3.10649.

Scaperdas, A. and Gilham, S., 2004. "Thematic Area 4: Best practice advice for civil construction and HVAC". *The QNET-CFD Network Newsletter*, Vol. 2, No. 4, pp. 28–33.

Tamura, Y., Xu, X., Tanaka, H., Kim, Y.C., Yoshida, A. and Yang, Q., 2017. "Aerodynamic and pedestrian-level wind characteristics of super-tall buildings with various configurations". *Procedia Eng.*, Vol. 199, pp. 28–37. ISSN 1877-7058. DOI 10.1016/j.proeng.2017.09.146.

Tannehill, J.C., Anderson, D.A. and Pletcher, R.H., 1997. *Computational Fluid Mechanics and Heat Transfer*. Series in Computational and Physical Processes in Mechanics and Thermal Sciences. Taylor & Francis Group, Washington, DC, 2nd edition. ISBN 9781560320463.

Vardoulakis, S., Fisher, B.E.A., Pericleous, K. and Gonzalez-Flesca, N., 2003. "Modelling air quality in street canyons: a review". *Atmos. Environ.*, Vol. 37, No. 2, pp. 155–182. ISSN 1352-2310. DOI 10.1016/S1352-2310(02)00857-9.

9. RESPONSIBILITY NOTICE

The authors are the only responsible for the printed material included in this paper.